

Cite this: *RSC Adv.*, 2017, 7, 6827

# Nanophasic morphologies as a function of the composition and molecular weight of the macromolecular cross-linker in poly(*N*-vinylimidazole)-*l*-poly(tetrahydrofuran) amphiphilic conetworks: bicontinuous domain structure in broad composition ranges†

Csaba Fodor,<sup>‡\*a</sup> Gergely Kali,<sup>§a</sup> Ralf Thomann,<sup>b</sup> Yi Thomann,<sup>b</sup> Béla Iván<sup>\*a</sup> and Rolf Mülhaupt<sup>b</sup>

Macroscopically homogeneous poly(*N*-vinylimidazole)-linked *by*-poly(tetrahydrofuran) (PVIIm-*l*-PTHF) amphiphilic conetworks (APCNs) were investigated to reveal the effect of conetwork composition in a broad composition range between 25–91 wt% PTHF content and the molecular weight of the components on phase separation and the formation of different morphological features. No macroscopic phase separation was found in these conetworks with semicrystalline PTHF phase, but the segregation of the various covalently connected phases occurs in the nanoscale. The nanophase separated APCNs possess compositionally asymmetric morphology with spherical and elongated domains together with a bicontinuous (cocontinuous) domain structure having ~7–19 nm average domain sizes. The molecular weight of the PTHFDMA cross-linker, varying between 2170 and 10 030 g mol<sup>-1</sup>, also influences the size and distance between the phases. Moreover, morphology dependent interactions with polar and non-polar solvents, as well as amphiphilic swelling behavior were found. These nanostructured materials, due to their unique nanophasic morphology and swelling properties possess significant importance and have numerous potential applications in various fields from medicine to material science and engineering.

Received 17th October 2016  
Accepted 19th December 2016

DOI: 10.1039/c6ra25356c

www.rsc.org/advances

## Introduction

The phase behaviour of bi- and multicomponent macromolecular assemblies composed of immiscible polymer chain segments has attracted considerable attention in diverse application fields of nanotechnology. These materials can spontaneously self-assemble into a rich variety of periodic patterns with dimensions in the nanometer range.<sup>1</sup> A mixture of homopolymers self-isolate into macroscopically separated polymer regions, while the covalently bonded polymer blocks

minimize their repulsive energy by micro- or nanophase segregation into various highly ordered morphologies. The morphology depends on the composition and molecular weight of the interconnected polymer chains. Both theoretical and experimental studies on binary block copolymer systems are well known, and strong tendency of composition dependent phase separation or formation of well-ordered nanostructures were found. The phases can form two types of spherical and cylindrical microstructures, depending on the composition, as well as lamellar morphology, or as complex phases, ordered bicontinuous double gyroid structure.<sup>2</sup> In more details, the theory of dynamics of block copolymer's self-assembly is described in the reviews by Bates and Fredrickson.<sup>3,4</sup>

Amphiphilic conetworks (APCNs) are nanophase separated soft materials, composed of covalently bonded, otherwise immiscible hydrophilic and hydrophobic (or even fluorophilic<sup>5–9</sup>) polymer chains.<sup>10–12</sup> In addition the chemically bonded APCNs, supramolecular amphiphilic gels consisting of trivalent polyisobutylene and bivalent poly(ethylene oxide)<sup>13</sup> and physically cross-linked gels *via* stereocomplex formation of two polylactide enantiomers<sup>14,15</sup> are also reported. These novel polymeric systems belong to a rapidly emerging class of materials and have sparked

<sup>a</sup>Polymer Chemistry Research Group, Institute of Materials and Environmental Chemistry, Research Centre for Natural Sciences, Hungarian Academy of Sciences, Magyar tudósok körútja 2, H-1117 Budapest, Hungary. E-mail: c.fodor@rug.nl; ivan.bela@ttk.mta.hu

<sup>b</sup>Freiburg Materials Research Center and Institute for Macromolecular Chemistry, University of Freiburg, Stefan-Meier-Straße 21, D-79104 Freiburg, Germany

† Electronic supplementary information (ESI) available: Supporting table and figures. See DOI: 10.1039/c6ra25356c

‡ Macromolecular Chemistry and New Polymeric Materials, Zernike Institute for Advanced Materials, University of Groningen, Nijenborgh 4, 9747 AG Groningen, The Netherlands.

§ Organic Macromolecular Chemistry, Saarland University, Campus C 4.2, 66123 Saarbrücken, Germany.

enormous interest in the last few decades in both pure and applied sciences.<sup>7,8,16–31</sup> APCNs possess several unique characteristics, such as the amphiphilic swelling properties and the improved mechanical characteristics compared to homopolymer hydrogels. Moreover, a special property of these materials is their phase behaviour. Indeed, in comparison with the different nanostructures and architectures of binary block copolymers, the nanophase APCNs possess compositionally asymmetrical morphology with a cocontinuous (bicontinuous) nanophase-separated structure over a broad composition range. The incompatibility of the different hydrophilic and hydrophobic polymer phases not only subserves the formation of co-(bi) continuous structures, but beyond the asymmetrical morphology development, spherical and coalesced elongated domains also appear. These domains have various proportions over the composition range and the phase separation in the APCNs leads to average domain sizes in the nanometer scale. Diversity of techniques involving differential scanning calorimetry (DSC),<sup>22,30</sup> small angle X-ray scattering (SAXS),<sup>20,24,27</sup> small angle neutron scattering (SANS),<sup>25,27</sup> transmission electron microscopy (TEM),<sup>17,19,27,30</sup> atomic force microscopy (AFM)<sup>17,19,30,32</sup> and solid-state NMR<sup>20,21</sup> were used to confirm the formation of separated nanodomains in these materials. The systematic study of the compositionally asymmetrical morphology of APCNs is of major importance, when a stable, bicontinuous nanophase-separated structure is formed over a broad composition window of both constituent phases with large inner surface between the distinct phases. This kind of morphology is favourable in a variety of fields such as ion conduction,<sup>33</sup> oxygen permeation,<sup>34,35</sup> tissue engineering<sup>36</sup> as well as support for enhanced enzyme catalysis<sup>18,19,37</sup> or nanotemplates of nanohybrid materials.<sup>27</sup>

In our previous publications, the synthesis and some fundamental structure–property correlations of poly(*N*-vinylimidazole) (PVIIm) based conetworks were investigated.<sup>22,38–41</sup> The widely used hydrophilic PVIIm was cross-linked by the biocompatible, hydrophobic, rubbery methacrylate-telechelic polytetrahydrofuran (PTHFDMA) macromonomer with well-defined molecular weights. It was recently demonstrated that the poly(*N*-vinylimidazole)-linked by-poly(tetrahydrofuran) (PVIIm-*l*-PTHF) amphiphilic conetworks with various PTHF lengths and different PVIIm/PTHF ratios have some unprecedented structure–property relations. These parameters influence the scissor effect of the macromolecular cross-linker on the glass transition temperature, which supports the correlations between the fundamental structural parameters and the glass transition temperatures of the components.<sup>22</sup> In this study, we aimed at to gain insight into the effect of composition and cross-linker on the nanophase separated morphology of the PVIIm-*l*-PTHF conetworks. Through this dependence, the other goal of this work is to reveal the relationship between the swelling behaviour and the structural parameters. Based on our systematic investigations, the findings and interpretations reported here provide valuable insights into several aspects of revealing and understanding the structure–property relationships and nanostructure formation in these novel, rapidly emerging soft materials.

## Experimental

### Materials

*N*-Vinylimidazole (VIm, ≥99%, Aldrich) was vacuum distilled from calcium hydride (CaH<sub>2</sub>, 95%, Aldrich) at 72 °C, and kept under nitrogen until used. Hydroxyl-ended poly(tetrahydrofuran) (Terathane 2000 polyether glycol, PTHFDOH, average  $M_n \sim 2000 \text{ g mol}^{-1}$ ) was purchased from Fluka. Triethylamine (Et<sub>3</sub>N, ≥99.5%) and methacryloyl chloride (MACl, ≥97%) were purchased from Fluka and were distilled under vacuum (Et<sub>3</sub>N room temperature, MACl 30–32 °C). Dichloromethane (DCM, 98%, Scharlau) was refluxed over CaH<sub>2</sub> (95%, Aldrich), and freshly distilled before use. *n*-Hexane (96%, Scharlau) was stored over concentrated sulfuric acid (Freak), then was passed through a basic aluminum oxide (99%, Aldrich) column to remove the acidic impurities. Finally, it was refluxed over CaH<sub>2</sub> and freshly distilled before use. Tetrahydrofuran (THF, Spektrum 3D) was purified by distillation over CaH<sub>2</sub>, and it was used directly after distillation. Trifluoromethanesulfonic anhydride (Tf<sub>2</sub>O, 99+%, Aldrich) was purified by vacuum distillation at 78 °C right before use. Sodium methacrylate (NaMA, 99%, Sigma) was used as received. Freshly distilled absolute ethanol (EtOH, Molar Chemicals) was used as a solvent for the copolymerization. Methanol (MeOH, 99.97%, Spectrum 3D) was used as received. Deionized water was applied for the purification of the polymers.

### Instruments and measurements

**Nuclear magnetic resonance (NMR).** <sup>1</sup>H NMR spectroscopy was used to obtain the chemical composition and the purity of the monomers and polymers utilized, both commercial and synthesized, in this research. <sup>1</sup>H NMR spectra were obtained on a Varian Unity INOVA spectrometer operating at <sup>1</sup>H frequency of 400 MHz. Samples were dissolved in appropriate deuterated solvents (chloroform-*d* or deuterated water). TMS at 0 ppm, CDCl<sub>3</sub> at 7.28 ppm, DHO at 4.79 ppm were used as internal references.

**Gel permeation chromatography (GPC).** The molecular weights and the polydispersities ( $\bar{D}$ ) of the polymers were determined by GPC using Polymer Laboratories Mixed C type column set with three columns in distilled THF with a flow rate of 1.0 mL min<sup>−1</sup>, and detection was carried out by a dual RI and viscosity detector (Viscotek Dual 200). Molecular weights and  $\bar{D}$  were calculated by the use of universal calibration made with 22 narrow  $\bar{D}$  polystyrene standards in the range of 104 to  $3 \times 10^6 \text{ g mol}^{-1}$ .

**Elemental analysis.** The composition of the conetworks was determined by elemental analysis with a Heraeus CHN-O-RAPID instrument. The chemical compositions were calculated from the atomic percentages of carbon, nitrogen, and hydrogen.

**Differential scanning calorimetry (DSC).** Calorimetric measurements were made on a Mettler TG50 instrument differential scanning calorimeter in a dry nitrogen atmosphere. The annealed samples were scanned in a temperature range from −120 °C to 200 °C by heating-cooling-heating scans with the heating-cooling rates of 10 °C min<sup>−1</sup> in all cases. The inflection point of the specific heat increase in the transition



region during the second heating scan is reported as the glass transition temperature ( $T_g$ ). The melting temperature ( $T_m$ ) was taken as the minimum of the endothermic peak.

**Atomic force microscopy (AFM).** AFM experiments were performed on a MultiMode scanning probe microscope with Nanoscope IIIa controller (Digital Instruments) at ambient condition in height and phase imaging modes. The flat cryo-sectioned surfaces of the annealed conetworks used for examination were obtained by using a Diatome diamond knife at  $-100\text{ }^\circ\text{C}$  using a Leica EMFCS microtome.

**Swelling measurements.** Swelling of the conetworks was determined gravimetrically in solvents with various polarities (THF, water). The experiments were carried out as follows: the conetwork samples were cut into small slabs, and the middle part of the hydrogel was used for the swelling experiments. The dried polymer samples were placed in the selected solvent at room temperature and were left to swell until constant weight. The samples were removed from the solvent, wiped with a filter paper and weighed. The equilibrium swelling ratios ( $Q$ ) were obtained at constant weight and calculated by the following relation:

$$Q = \frac{m - m_0}{m_0}$$

where  $m$  and  $m_0$  are the weights of the swollen and the dry conetworks, respectively.

## Synthetic procedures

**Poly(tetrahydrofuran)-dimethacrylate (PTHFDMA) cross-linker synthesis.** Macromonomers were synthesized following previously published protocols.<sup>22</sup> Briefly, low molecular weight methacrylate-telechelic PTHF cross-linker was synthesized as follows: hydroxyl-ended PTHF (0.01 mol) was dissolved in DCM and then freshly distilled MACl (10 mmol), and  $\text{Et}_3\text{N}$  (0.10 mol) was added at  $-50\text{ }^\circ\text{C}$  under an inert atmosphere and permanent stirring. After overnight reaction and methanol addition, the solvent was evaporated, and the polymer was precipitated into  $n$ -hexane. The redissolved product in was washed with water and dried. The efficiency of the end-group modification and the molecular weight of the product were confirmed by  $^1\text{H}$  NMR and GPC ( $M_n(\text{NMR}) = 2170\text{ g mol}^{-1}$ ,  $F_n = 1.98$ ,  $M_n(\text{GPC}) = 2570\text{ g mol}^{-1}$ ,  $D = 1.65$ );  $^1\text{H}$  NMR (400 MHz, chloroform- $d$ ):  $\delta$  1.60 (4H, s), 1.93 (6H, s), 3.41 (4H, s), 4.15 (4H, t,  $J = 6.4\text{ Hz}$ ), 5.51 (2H, s), 6.07 (2H, s).

Synthesis of the higher molecular weight PTHFDMA macro-cross-linkers proceeds as follows: freshly distilled  $\text{TiF}_2\text{O}$  initiator (2.48 mmol) was added to distilled THF (2.48 mol) under permanent stirring. *In situ* termination and functional group modification was performed by adding chloroform suspension of NaMA (24.8 mmol) to the reaction mixture after pre-determined time. After 48 hour reaction time the solvent was evaporated, and the polymer was precipitated into water/methanol (1/1). The crude product was redissolved in THF filtered through aluminum oxide and silica gel column and concentrated. The molecular weights and the end-group modification efficiency were confirmed by  $^1\text{H}$  NMR and GPC ( $M_n(\text{NMR}) = 6850\text{ g mol}^{-1}$ ,  $F_n = 1.99$ ,  $M_n(\text{GPC}) = 8650\text{ g mol}^{-1}$ ,

$D = 1.19$  for PTHF6.8kDMA and  $M_n(\text{NMR}) = 10\,030\text{ g mol}^{-1}$ ,  $F_n = 1.97$ ,  $M_n(\text{GPC}) = 11\,550\text{ g mol}^{-1}$ ,  $D = 1.21$  for PTHF10kDMA);  $^1\text{H}$  NMR (400 MHz, chloroform- $d$ ):  $\delta$  1.61 (4H, s), 1.93 (6H, s), 3.40 (4H, s), 4.15 (4H, t,  $J = 6.4\text{ Hz}$ ), 5.53 (2H, s), 6.08 (2H, s).

**Preparation of poly(*N*-vinylimidazole)-*l*-poly(tetrahydrofuran) conetworks (P2.2k, P6.8k, and P10k).** The APCN samples were prepared as described previously.<sup>22</sup> Briefly, the conetworks were synthesized as follows: determined amounts of cross-linking agent and comonomer, initiator and common solvent for all components were measured into glass vials homogenized, deoxygenated by nitrogen purging and transferred into Teflon molds in an AtmosBag<sup>TM</sup> (Sigma-Aldrich) under nitrogen atmosphere. The closed molds were kept in an oven at  $65\text{ }^\circ\text{C}$  for 72 hours. Subsequently, the molds were cooled to room temperature, the solvent was evaporated, the conetworks dried under vacuum and the resulting conetworks were extracted with polar (MeOH) and non-polar (THF) solvents and the extractables were determined gravimetrically with some exception around and below 15%. The composition of the conetworks was determined by elemental analysis and varied between 25–89 wt%, 52–84 wt% and 46–91 wt% PTHF content, for cross-linkers with molecular weights of 2170, 6850 and  $10\,030\text{ g mol}^{-1}$ , respectively.

**Annealing of the poly(*N*-vinylimidazole)-*l*-poly(tetrahydrofuran) (PVIm-*l*-PTHF) conetworks.** Heat treatment was achieved on the small pieces of the dried conetworks with *ca.* 2–3 mm thickness. The samples were annealed under nitrogen atmosphere at a high temperature ( $200\text{ }^\circ\text{C}$ ) in a vacuum oven for 5 h. The temperature was increased stepwise and after heat treatment, the samples were let slowly cool down. The treated conetworks were investigated by atomic force microscopy (AFM) measurements.

**Symbolism used.** The notation of the APCNs follows by their chemical constituents: the symbols first show the  $M_n \times 10^{-3}$  of the hydrophobic PTHF macromonomer cross-linker, followed by the hydrophobic PTHF content (wt%). For example, P2.2k-25 stands for conetwork consisting PTHF cross-linker of  $M_n\,2170\text{ g mol}^{-1}$  with a PTHF content of 25 wt%.

## Results and discussion

A series of PVIm-*l*-PTHF conetworks used in this study were synthesized *via* free radical copolymerization of the PTHFDMA macromonomer and the VIm comonomer. For the conetwork preparations, PTHF cross-linkers with various molecular weights ( $M_n = 2170, 6850$  and  $10\,030\text{ g mol}^{-1}$ ) and near to quantitative endfunctionalities ( $F_n \sim 2$ ) were produced and utilized. Conetworks of this macro-cross-linker and VIm were formed in a broad composition range from 25 to 91 wt% PTHF content (see ESI† for feed ratios and composition details). The synthesis route and the resulting cross-linked polymer structure of the PVIm-*l*-PTHF conetworks are depicted in Fig. 1.

Based on our previous work on these materials, phase separation is expected in the transparent PVIm-*l*-PTHF conetworks between the incompatible, but covalently connected polymer chains. This phenomenon was proved by DSC<sup>22</sup> and solid-state NMR investigations,<sup>38</sup> by which two separate glass transitions were found in the conetworks (Fig. 2), indicating immiscibility of the components. It was also demonstrated that





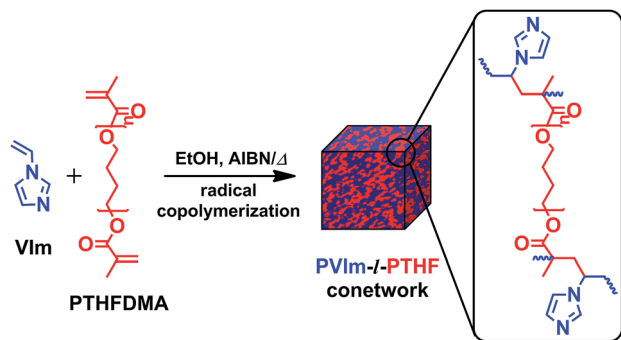


Fig. 1 Schematic representation of the synthesis and structure of poly(*N*-vinylimidazole)-*l*-poly(tetrahydrofuran) (PVIm-*l*-PTHF) conetworks. The colors in the conetwork structure represent hydrophobic PTHF (red) and hydrophilic PVIm (blue).

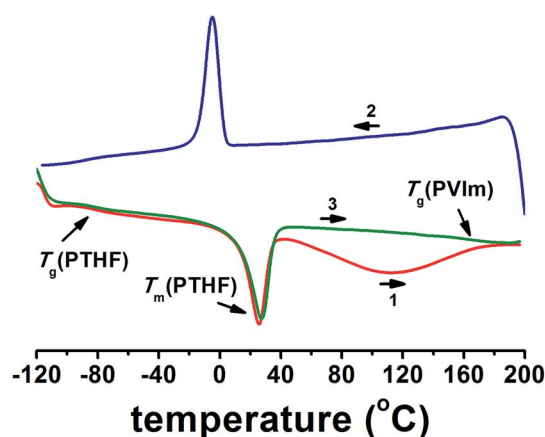


Fig. 2 Differential scanning calorimetry (DSC) thermograms (first heating (1), cooling (2) and second heating (3) cycles) of poly(*N*-vinylimidazole)-*l*-poly(tetrahydrofuran) (PVIm-*l*-PTHF) conetwork (P10k-62 sample;  $T_g(\text{PVIm}) = 158^\circ\text{C}$ ,  $T_g(\text{PTHF}) = -86^\circ\text{C}$ ,  $T_m(\text{PTHF}) = 27^\circ\text{C}$ ).

the glass transition temperatures changed with the composition of the conetworks and the molecular weight of PTHF cross-linkers.<sup>22</sup> Since these immiscible components are covalently connected to each other, the macroscopic demixing is prohibited. Separation of the two phases can occur only in the

nanoscale, confirmed by the optical transparency of the conetworks. For surface and bulk morphology examination, phase imaging by AFM or scanning probe microscopy is a convenient method, which provides valuable structural information.

Bulk morphology of the flat cryo-sectioned, annealed PVIm-*l*-PTHF conetworks was investigated. Phase mode AFM was performed at ambient condition that is above the melting point and glass transition temperature of PTHF, to determine the morphology and the dimensions of the phases. Representative AFM phase mode images of nanophase separated conetworks with various PTHF contents are shown in Fig. 3 (details of the AFM phase images for the whole conetwork series are presented in the ESI, see Fig. S1–S3†). For the correct interpretation of the phase mode AFM images, it is crucial to remark that cantilever with a tip curvature between 2–5 nm was used to get the necessary lateral resolution and identify the structure size as small as a few nanometers. The contrast, namely the diffuse tone difference between the phases in the phase mode AFM images can be used to map the variations of the distinct material properties, such as surface elasticity, and the direct visualization of the morphology. In the AFM phase images the two distinct polymer nanophases in the conetworks, specifically the glassy, hydrophilic PVIm and the elastic, soft PTHF phase appear with different colors, light and dark brown, respectively.

The cross-section analysis allows obtaining characteristic information about the bulk morphology of the conetworks. The AFM images indicate in all cases nanophase separation of the two polymers with different philicities, but the domains do not organize in a regular lattice over the whole composition range due to the randomly cross-linked structure of the conetworks.<sup>20,27</sup> At low cross-linker content, (P2.2k-25 and P6.8k-52) the hydrophobic PTHF domains are dispersed in the continuous hydrophilic PVIm matrix as spheres. At increased hydrophobic ratio (P2.2k-38 and P10k-46) the distortion of the spherical domains is noticeable and elongated structures arise. From 47 wt%, 61 wt% and 66 wt% PTHF cross-linker content, depending on the molecular weight of the macromonomer (2.2k, 6.8k or 10k, respectively) the elongated PTHF phases interconnect to form continuous, more precisely cocontinuous (bicontinuous) phase next to the extended PVIm. The AFM micrographs of the PVIm-*l*-PTHF conetworks clearly indicate that in the conetworks the two incompatible hydrophilic and

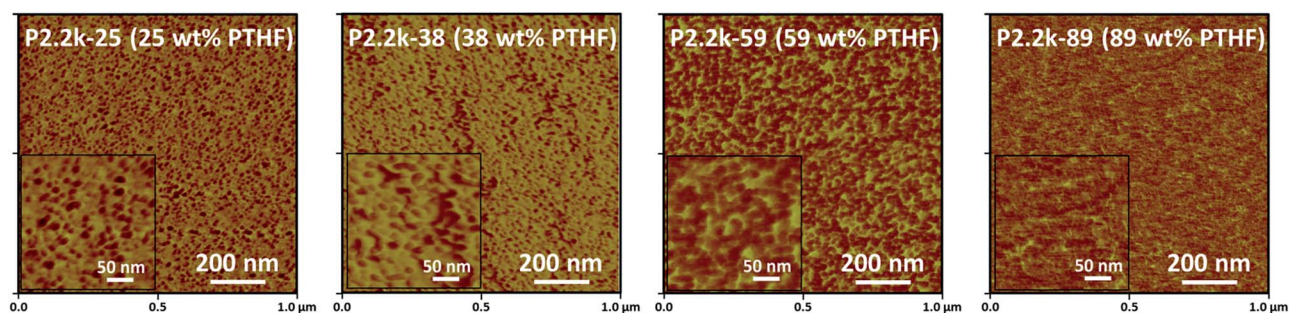


Fig. 3 Representative phase mode AFM images of cross sections of poly(*N*-vinylimidazole)-*l*-poly(tetrahydrofuran) (PVIm-*l*-PTHF) conetwork samples with different compositions. Inset: AFM image magnification of conetwork samples (the softer PTHF phase appears dark and the harder PVIm is bright).



hydrophobic polymers exist in continuous phases next to each other. This bicontinuous phase morphology appears in a broad composition range, from 47 to 86 wt% PTHF content, with varying PTHF cross-linker molecular weights. At relatively high PTHF content the PVIm phases are interconnected with a certain extent and appear as nerve like system in the disordered continuous hydrophobic PTHF matrix.

It should be noted that the surface morphology may differ from the bulk morphology of the conetworks, due to the enrichment of one component on the surface during the synthesis of the conetwork.<sup>42</sup> In other words, in PVIm-*l*-PTHF conetworks the hydrophobic polymer segments will move toward the surface, whereas the polymer segments with opposite philicity will become buried in the bulk, to minimize the surface energy. The selective separation of one component on surfaces was investigated and verified by Bruns *et al.* by applying surfaces with different chemical nature (poly(propylene), glass, Teflon, and argon) on 2-hydroxyethyl acrylate based conetworks.<sup>43</sup>

In binary block copolymers, the blocks are chemically bonded to each other, resulting in some degree of incompatibility and separating into microphases. In order to minimize the evolving incompatibility of the blocks, the copolymers self-assemble into various phase structures, as shown in Fig. 4. According to the theoretical phase diagram of block copolymers, the corresponding morphologies for binary block copolymers are indicated as follows: spheres, cylinders, gyroid and lamellar with increasing volume fraction of one of the polymer blocks. The bicomponent conetworks, compared to the binary block copolymers, have compositionally asymmetrical morphology with analogous phase structures from spherical to

stable bicontinuous phase morphology. This phase behavior appears in a broad composition range and at high polymer B content reversed elongated/spherical domains are formed (Fig. 4).

The good quality and contrast of the AFM images (Fig. 3 and S2–S4†) allow qualitative evaluation of the PTHF domain sizes, *i.e.* the diameter of the hydrophobic domains and the inter-domain distances between the PTHF phases (details are presented in the ESI, see Fig. S5–S10†). The results reveal that the distribution of the domain sizes and inter-domain distances in the investigated PVIm-*l*-PTHF conetwork samples are unexpectedly narrow. The determined PTHF domain sizes of the APCNs vary between 7 nm and 19 nm while the PTHF inter-domain distances are in the range of 15 nm to 28 nm as shown in Fig. 5. It can be clearly seen in this figure that with higher molecular weight PTHF cross-linker the formed phases in the conetworks, as well as the distances, become larger than in the case of the short macromonomers (P2.2k). The hydrophilic phase sizes are in the range from 3 nm to 10 nm, which is in a good correlation with the average molecular weights of the hydrophilic PVIm segments between two cross-linking points ( $M_c$ ) which vary between 134 and 5870 g mol<sup>−1</sup>.<sup>22</sup>

To study the correlation between different morphological features and the swelling behaviour of PVIm-*l*-PTHF conetworks, swelling measurements were performed. In particular, swelling studies on the conetworks with various composition, cross-linker length, therefore with different morphology, were carried out in water and THF. The data in Fig. 6 show the equilibrium swelling ratios ( $Q$ ) as a function of composition (wt% PTHF content), and the compositionally asymmetrical

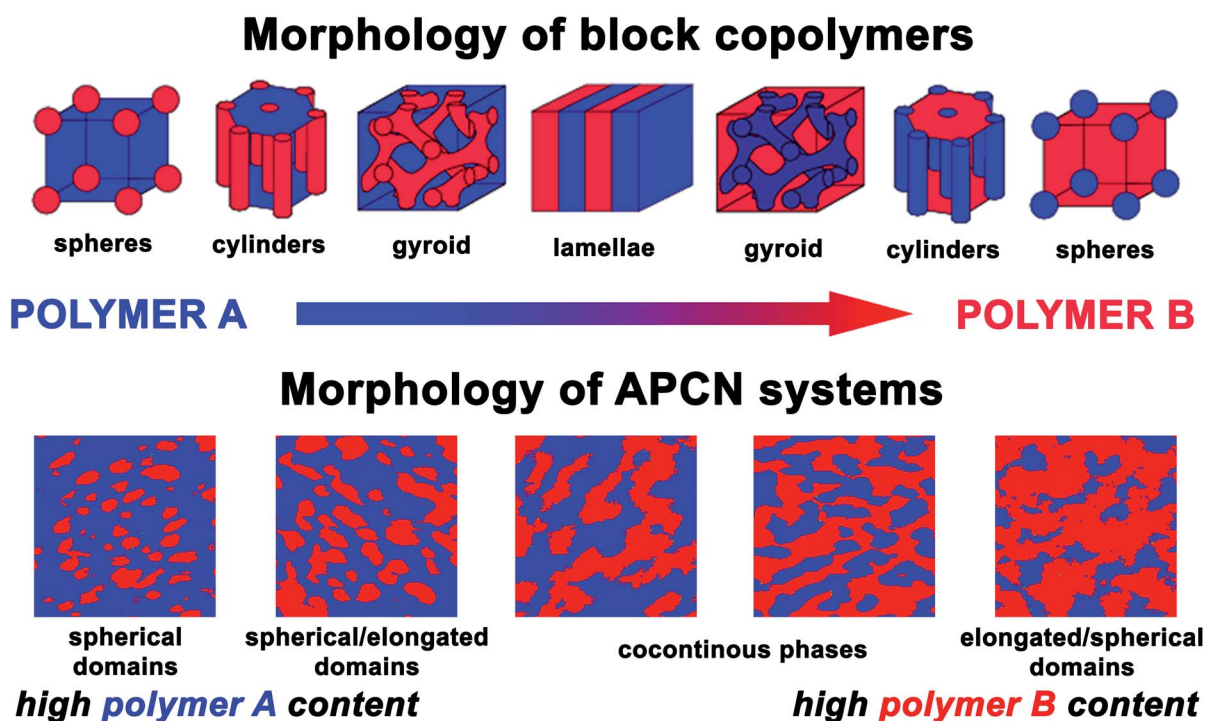


Fig. 4 Comparison of the morphological arrangements of the immiscible components of A–B diblock copolymers with the compositionally asymmetrical nanophasic morphology of amphiphilic polymer conetworks.



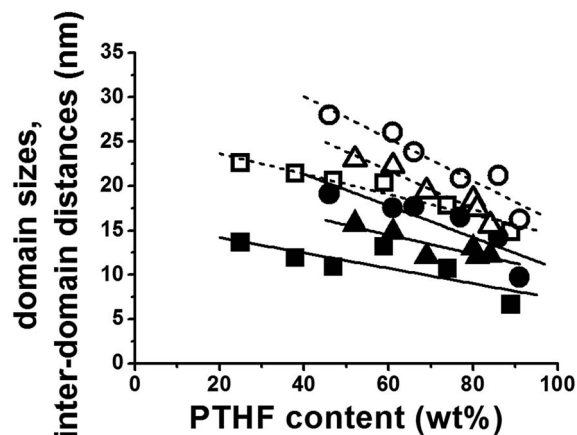


Fig. 5 Average poly(tetrahydrofuran) (PTHF) domain sizes (closed symbols) and average PTHF inter-domain distances (open symbols) determined by phase mode AFM of the poly(*N*-vinylimidazole)-*l*-poly(tetrahydrofuran) (PVIm-*l*-PTHF) conetwork with varying PTHF content: (■, □) for P2.2k, P6.8k (●, ○) and (▲, △) for P10k conetwork series.

morphology of the conetworks are also depicted in this figure. The  $Q$  values for both solvents change with the composition, *i.e.* the higher the PVIm/PTHF ratio in the conetworks, the higher the swelling in aqueous solutions. The swelling in the nonpolar THF follows opposite tendency, confirming that the increased hydrophobic ratio subserves the nonpolar swelling. In other words, the PVIm-*l*-PTHF conetworks behave as hydrogels in polar and as hydrophobic gels in nonpolar solvents, meaning that the conetworks possess amphiphilic character. At low PTHF content, mostly isolated spherical PTHF domains are present in the continuous PVIm phase, and the swelling of the conetwork in nonpolar solvents is restricted by the non-swollen, rigid hydrophilic matrix. With higher PTHF content the hydrophobic swelling becomes more pronounced, due to the diminished integrity of the glassy phase by the coalesced PTHF domains, shown in Fig. S1.† In this case, the expansion capacity of the PTHF domains is greater in the coherent non-swollen PVIm phase, thus the swelling in THF is more feasible. In a relatively broad composition range, where the bicontinuous phase morphology emerges, both nonpolar and polar swelling occurs with nearly the same ratio. The coexistence of the separately coherent phases allows the interaction with solvents with different polarity, and the swelling is limited only by the PVIm/PTHF ratio in the conetworks. During the swelling, the appropriately swollen phase can change the conformation or even stretch the surrounding non-swollen phase. This forced non-equilibrium state of the solvent non-compatible phase in the cocontinuous APCN is preserved during the swelling, due to the cross-linked structure.<sup>24,27,38</sup> With increasing hydrophobic content the swelling tendency reverses. The predominant hydrophobic phase facilitates the swelling in nonpolar solvents, while the smaller and isolated PVIm phases in the coherent PTHF matrix are not able to force the whole conetwork to swell. The arrangement of the PVIm phase in the structure is similar to a nerve system with thin walls among the continuous

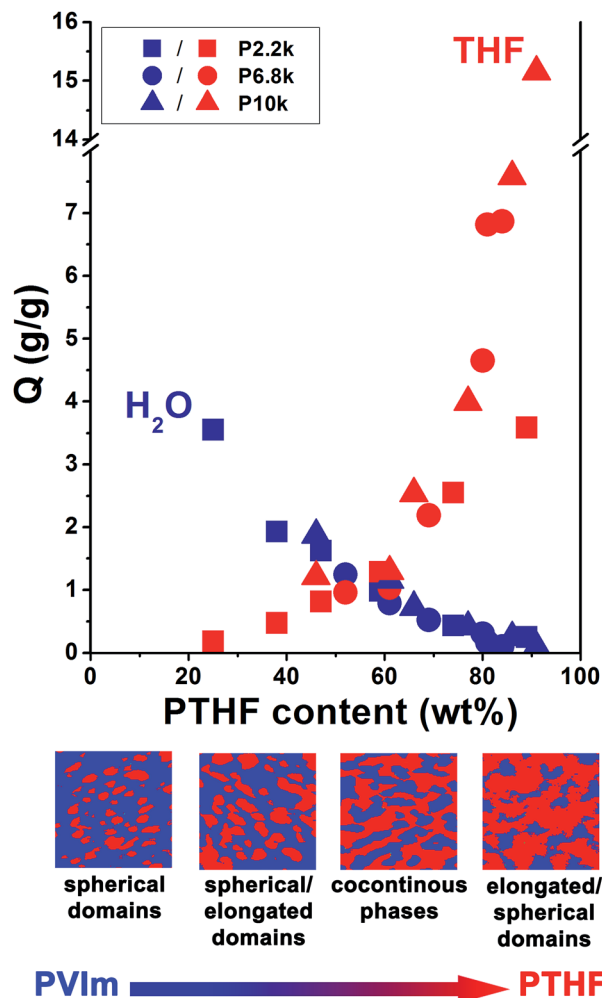


Fig. 6 Correlation between composition, morphological features and swelling of the poly(*N*-vinylimidazole)-*l*-poly(tetrahydrofuran) (PVIm-*l*-PTHF) conetwork series: equilibrium swelling ratios ( $Q$ ) in THF and distilled water as a function of the PTHF content and the morphology of the PVIm-*l*-PTHF conetworks.

polymer matrix. For the samples with high cross-linker content and distinct elongated/spherical PVIm domains, the aqueous swelling is negligible, while the hydrophobic swelling reaches enormous ratios (up to ~1500%) with PTHF content around 91 wt%.

The swelling is not only affected by the morphology that is related to composition, but it seems that molecular weight of the cross-linker influences also the nonpolar swelling of the APCNs. In the case of higher molecular weight cross-linker sample, within the same composition range, the nonpolar swelling is slightly higher. The difference in the swelling is most likely due to the structural differences in the conetwork samples, such as the cross-link density or the spatial gel inhomogeneities (caused *e.g.* by permanent entanglements, loops, or even dangling/unreacted chain ends). In the case of the low molecular weight cross-linkers, the samples possess higher cross-link density compared to the conetworks formed from longer PTHF cross-linkers, which might restrict the polymer segment mobility.





## Conclusions

In summary, it can be concluded on the basis of our systematic investigations by AFM and swelling experiments with a series of transparent, macroscopically homogenous poly(*N*-vinylimidazole)-linked by-poly(tetrahydrofuran) (PVIm-*l*-PTHF) amphiphilic conetworks that disordered bicontinuous nanophase separated morphology with ~7–19 nm domain sizes exist in these conetworks in a broad composition range. Compositionally asymmetrical morphologies and cocontinuous nanophase separated structures were revealed over a wide compositional window, affected by the composition and length of the macromonomer. With the variation of the molecular weight of the PTHF cross-linkers, control over the sizes and distances of the domains can be achieved. Additionally, the comparison of the conetworks' morphology with the swelling behavior showed morphology dependent interaction of the amphiphilic gels with polar and non-polar solvents.

## Acknowledgements

The authors are grateful for the NMR measurements, elemental and thermal analyses to A. Domján, H. Medzihradszky-Schweiger, and J. Szauer, respectively. Partial support of this research by the National Research, Development and Innovation Office (OTKA K112094) and the National Development Agency (KTIA-AIK-12-1-2012-0014) is also acknowledged.

## Notes and references

- 1 I. W. Hamley, *The physics of block copolymers*, Oxford University Press, New York, 1998.
- 2 M. Muthukumar, C. K. Ober and E. L. Thomas, *Science*, 1997, **277**, 1225–1232.
- 3 F. S. Bates and G. H. Fredrickson, *Annu. Rev. Phys. Chem.*, 1990, **41**, 525–557.
- 4 G. H. Fredrickson and F. S. Bates, *Annu. Rev. Mater. Res.*, 1996, **26**, 501–550.
- 5 N. Bruns and J. C. Tiller, *Macromolecules*, 2006, **39**, 4386–4394.
- 6 Z. Hu, L. Chen, D. E. Betts, A. Pandya, M. A. Hillmyer and J. M. DeSimone, *J. Am. Chem. Soc.*, 2008, **130**, 14244–14252.
- 7 Y. Wang, D. E. Betts, J. A. Finlay, L. Brewer, M. E. Callow, J. A. Callow, D. E. Wendt and J. M. DeSimone, *Macromolecules*, 2011, **44**, 878–885.
- 8 Y. Wang, J. A. Finlay, D. E. Betts, T. J. Merkel, J. C. Luft, M. E. Callow, J. A. Callow and J. M. DeSimone, *Langmuir*, 2011, **27**, 10365–10369.
- 9 J. S. Zigmund, K. A. Pollack, S. Smedley, J. E. Raymond, L. A. Link, A. Pavia-Sanders, M. A. Hickner and K. L. Wooley, *J. Polym. Sci., Part A: Polym. Chem.*, 2016, **54**, 238–244.
- 10 G. Erdödi and J. P. Kennedy, *Prog. Polym. Sci.*, 2006, **31**, 1–18.
- 11 L. Mespouille, J. L. Hedrick and P. Dubois, *Soft Matter*, 2009, **5**, 4878–4892.
- 12 C. S. Patrickios and T. K. Georgiou, *Curr. Opin. Colloid Interface Sci.*, 2003, **8**, 76–85.
- 13 W. H. Binder, L. Petraru, T. Roth, P. W. Groh, V. Pálfi, S. Kéki and B. Iván, *Adv. Funct. Mater.*, 2007, **17**, 1317–1326.
- 14 X. Fan, M. Wang, D. Yuan and C. He, *Langmuir*, 2013, **29**, 14307–14313.
- 15 Z. Li, B. H. Tan, T. Lin and C. He, *Prog. Polym. Sci.*, 2016, **62**, 22–72.
- 16 J. W. Bartels, P. M. Imbesi, J. A. Finlay, C. Fidge, J. Ma, J. E. Seppala, A. M. Nystrom, M. E. Mackay, J. A. Callow, M. E. Callow and K. L. Wooley, *ACS Appl. Mater. Interfaces*, 2011, **3**, 2118–2129.
- 17 N. Bruns and J. C. Tiller, *Nano Lett.*, 2005, **5**, 45–48.
- 18 S. Dech, T. Cramer, R. Ladisch, N. Bruns and J. C. Tiller, *Biomacromolecules*, 2011, **12**, 1594–1601.
- 19 S. Dech, V. Wruk, C. P. Fik and J. C. Tiller, *Polymer*, 2012, **53**, 701–707.
- 20 A. Domján, G. Erdödi, M. Wilhelm, M. Neidhöfer, K. Landfester, B. Iván and H. W. Spiess, *Macromolecules*, 2003, **36**, 9107–9114.
- 21 A. Domján, P. Mezey and J. Varga, *Macromolecules*, 2012, **45**, 1037–1040.
- 22 C. Fodor, A. Domján and B. Iván, *Polym. Chem.*, 2013, **4**, 3714–3724.
- 23 M. C. Hacker, A. Haesslein, H. Ueda, W. J. Foster, C. A. Garcia, D. M. Ammon, R. N. Borazjani, J. F. Kunzler, J. C. Salamone and A. G. Mikos, *J. Biomed. Mater. Res.*, 2009, **88**, 976–989.
- 24 G. Kali, T. K. Georgiou, B. Iván, C. S. Patrickios, E. Loizou, Y. Thomann and J. C. Tiller, *Macromolecules*, 2007, **40**, 2192–2200.
- 25 E. J. Kepola, E. Loizou, C. S. Patrickios, E. Leontidis, C. Voutouri, T. Stylianopoulos, R. Schweins, M. Gradzielski, C. Krumm, J. C. Tiller, M. Kushnir and C. Wesdemiotis, *ACS Macro Lett.*, 2015, **4**, 1163–1168.
- 26 C. Lin and I. Gitsov, *Macromolecules*, 2010, **43**, 10017–10030.
- 27 J. Scherble, R. Thomann, B. Iván and R. Mülhaupt, *J. Polym. Sci., Part B: Polym. Phys.*, 2001, **39**, 1429–1436.
- 28 K. Schöller, S. Küpfer, L. Baumann, P. M. Hoyer, D. de Courten, R. M. Rossi, A. Vetushka, M. Wolf, N. Bruns and L. J. Scherer, *Adv. Funct. Mater.*, 2014, **24**, 5194–5201.
- 29 C. N. Tironi, R. Graf, I. Lieberwirth, M. Klapper and K. Müllen, *ACS Macro Lett.*, 2015, **4**, 1302–1306.
- 30 J. Tobis, L. Boch, Y. Thomann and J. C. Tiller, *J. Membr. Sci.*, 2011, **372**, 219–227.
- 31 J. Xu, X. Li and F. Sun, *Drug Delivery*, 2011, **18**, 150–158.
- 32 B. Iván, M. Haraszti, G. Erdödi, J. Scherble, R. Thomann and R. Mülhaupt, *Macromol. Symp.*, 2005, **227**, 265–274.
- 33 C. N. Walker, K. C. Bryson, R. C. Hayward and G. N. Tew, *ACS Nano*, 2014, **8**, 12376–12385.
- 34 H. Sugimoto, G. Nishino, N. Tsuzuki, K. Daimatsu, K. Inomata and E. Nakanishi, *Colloid Polym. Sci.*, 2012, **290**, 173–181.
- 35 J. Xu, M. Qiu, B. Ma and C. He, *ACS Appl. Mater. Interfaces*, 2014, **6**, 15283–15290.
- 36 Y. Sun, J. Maughan, R. Haigh, S. A. Hopkins, P. Wyman, C. Johnson, N. J. Fullwood, J. Ebdon, S. MacNeil and S. Rimmer, *Macromol. Symp.*, 2007, **256**, 137–148.



- 37 N. Bruns, W. Bannwarth and J. C. Tiller, *Biotechnol. Bioeng.*, 2008, **101**, 19–26.
- 38 A. Domján, C. Fodor, S. Kovács, T. Marek, B. Iván and K. Süvegh, *Macromolecules*, 2012, **45**, 7557–7565.
- 39 C. Fodor, J. Bozi, M. Blazsó and B. Iván, *RSC Adv.*, 2015, **5**, 17413–17423.
- 40 C. Fodor and B. Iván, *J. Polym. Sci., Part A: Polym. Chem.*, 2011, **49**, 4729–4734.
- 41 C. Fodor, G. Kali and B. Iván, *Macromolecules*, 2011, **44**, 4496–4502.
- 42 D. Park, B. Keszler, V. Galiatsatos and J. P. Kennedy, *J. Appl. Polym. Sci.*, 1997, **66**, 901–910.
- 43 N. Bruns, J. Scherble, L. Hartmann, R. Thomann, B. Iván, R. Mülhaupt and J. C. Tiller, *Macromolecules*, 2005, **38**, 2431–2438.

